J Vet Intern Med 2005;19:15–22

Comparison of Ultrasonography, Computed Tomography, and Single-Photon Emission Computed Tomography for the Detection and Localization of Canine Insulinoma

Joris H. Robben, Yvonne W.E.A. Pollak, Jolle Kirpensteijn, Susanne A.E.B. Boroffka, Ted S.G.A.M. van den Ingh, Erik Teske, and George Voorhout

Accurate preoperative detection, localization, and staging of the primary tumor and metastases are essential for the selection of appropriate candidates for surgery. In dogs with insulinoma, preoperative assessment usually is performed with transabdominal ultrasonography (US). There are no reports on the use of computed tomography (CT) for this purpose. The preoperative use of somatostatin receptor scintigraphy (SRS) recently has been advocated for the identification of insulinoma and gastrinoma in dogs, but its accuracy remains to be established. In this report US, CT, and single-photon emission computed tomography (SPECT) with [^{111}In-DTPA-D-Phe^{1}]-octreotide (a specific form of SRS) were compared for their effectiveness in detecting and localizing primary and metastatic insulinoma in dogs. Findings at surgery or postmortem examination served as control. Of 14 primary insulinomas, 5, 10, and 6 were correctly identified by US, CT, and SPECT, respectively. No lymph node metastases were detected by US or SPECT. CT identified 2 of 5 lymph node metastases but also identified 28 false-positive lesions. Two of 4 livers were found to be positive for metastases by 1 of the imaging techniques. US can be used for the initial evaluation of dogs with hypoglycemia. Although CT identifies most primary tumors, intraoperative inspection and palpation of the pancreas is still superior. SPECT appears as effective as US and CT in detecting insulinomas. Future developments in preoperative imaging techniques might improve current methods of canine insulinoma detection.

Key words: Abdominal ultrasonography; Computed tomography; Diagnostic imaging; Dog; Pancreatic endocrine tumor; Somatostatin receptor scintigraphy.

Insulin-producing pancreatic endocrine tumor, or insulinoma, is the most common of the 3 types of pancreatic endocrine tumor (PET) described in the dog (insulinoma, gastrinoma, and glucagonoma).[1–3] Over 95% of insulinomas in dogs are malignant, and 40–50% have visibly metastasized at the time of surgery.[2,4,5] Insulinomas are identified and staged by means of preoperative transabdominal ultrasonography (US) and, to a lesser extent, by computed tomography (CT) and by inspection and palpation during exploratory laparotomy.

Data on the effectiveness of preoperative imaging techniques in dogs with insulinoma are limited to uncontrolled studies of transabdominal US.[6–8] In human medicine, several imaging techniques have been described and evaluated for preoperative identification and staging of PETs. Somatostatin receptor scintigraphy (SRS) has become an important and often 1st-line imaging method in humans with malignant PETs.[9–12] This imaging modality has a high sensitivity and a high specificity.[13–15] Additional advantages of this technique are whole-body scanning for extra-abdominal metastases, gamma probing for intraoperative identification of tumor foci, and selection of subjects suitable for treatment with a radiolabeled somatostatin analogue.[13,16] Recently, the use of SRS with [^{111}In-DTPA-D-Phe^{1}]-octreotide was described for identification of insulinomas and gastrinomas in dogs, but the diagnostic accuracy of this method in dogs has yet to be established.[17–19]

The purpose of this study was to compare transabdominal US, CT, and single-photon emission computed tomography (SPECT), a specific form of SRS, for their effectiveness in identifying primary tumors and metastatic disease in dogs with insulinoma.

Materials and Methods

Dogs

The dogs with insulinoma included in this study were presented at the Department of Clinical Sciences of Companion Animals of Utrecht University from 1998 to 2001. Not all eligible dogs were enrolled because of scheduling conflicts or lack of owner consent. Transabdominal US was performed as part of the routine diagnostic workup. Inclusion criteria included CT and SPECT and verification of localization, lesion size, and stage at surgery or postmortem examination within 4 weeks of these diagnostic studies. Histology results had to be available.

Food was withheld from all dogs 6 h before CT and SPECT, which were performed consecutively. The dogs were premedicated with medetomidine[a] IV, and anesthesia was induced with propofol[b] administered IV to effect. The trachea was intubated, and anesthesia during CT was maintained with inhalational isoflurane[c] vaporized in nitrous oxide/oxygen in a circle breathing system. Anesthesia was maintained with a continuous infusion of propofol during SPECT. At the start of anesthesia, a urinary catheter was placed in the bladder, and urine was collected in a closed system.

Surgery was performed by 1 of the authors who is an ACVS board-certified surgeon (JK). The surgeon was not blinded to the results of the imaging studies. After a routine exploratory celiotomy, the pancreas was visualized and palpated for evidence of primary or metastatic disease. Primary tumors were removed by a marginal suture fracture technique. Thorough exploration of the draining lymph nodes and liver by visualization and palpation was performed; abnormal lymph nodes were removed by complete excision or were biopsied. Suspected liver metastases were removed if possible or biopsied. Information on tumor localization obtained at surgery was considered

From the Departments of Clinical Sciences of Companion Animals (Robben, Pollak, Kirpensteijn, Teske), Diagnostic Imaging (Boroffka, Voorhout), and Pathology (van den Ingh), Faculty of Veterinary Medicine, Utrecht University, Utrecht, The Netherlands.

Reprint requests: J.H. Robben, Department of Clinical Sciences of Companion Animals, Faculty of Veterinary Medicine, Utrecht University, P.O. Box 80.154, NL-3508 TD Utrecht, The Netherlands; e-mail: J.H.Robben@vet.uu.nl.

Submitted January 21, 2004; Revised June 1, 2004; Accepted September 10, 2004.

Copyright © 2005 by the American College of Veterinary Internal Medicine

0891-6640/05/1901-0002/$3.00/0

accurate if plasma glucose concentrations performed 3 months after removal of the tumor were within the normal reference range after an overnight fast. Normal glucose concentrations suggested that no macroscopic tumor lesions were missed at surgery. Postmortem examinations were performed by 1 of the authors who is an ECVP board-certified pathologist (TSGAMvdI). The pathologist was blinded to the results of the imaging studies. The maximal diameter (md) of the tumor was measured in 3 perpendicular directions with a ruler during surgery or at postmortem examination (md-Control).

The Research Committee of the Department of Clinical Sciences of Companion Animals of Utrecht University approved the studies, and owner consent was obtained before enrollment.

Transabdominal Ultrasonography

Ultrasonographic examination of the abdomen was performed with a high-definition ultrasound system[d] equipped with broad-band phased array transducers (5–3 and 7–4 MHz). US examinations were performed by 1 of 2 of the authors (SAEBB or GV), both European specialists in veterinary diagnostic imaging. The transabdominal US examination was performed with the dogs in dorsal and lateral recumbency. The regions dorsal and dorsomedial to the descending duodenum, right of the portal vein, and immediately ventral to the right kidney were scanned for the right pancreatic lobe. The pancreaticoduodenal vein, which runs through the right pancreatic lobe parallel to the descending duodenum, also aided localization. The region ventral to the portal vein was scanned for the pancreatic corpus. For examination of the left pancreatic lobe, the region caudal to the cranial duodenal flexure and greater curvature of the stomach, left of the portal vein, was scanned. The splenic vein, which passes caudodorsally to the left pancreatic lobe, was identified to aid localization. The liver and the regions of the pancreaticoduodenal, gastric, jejunal, splenic, and hepatic lymph nodes were carefully examined for possible metastases. The maximal diameters of the primary pancreatic lesion and metastatic lesions, if present (md-US), were measured along 2 or, if possible, 3 perpendicular axes. The written reports and video recordings of the US studies were reviewed by 1 of the authors (SAEBB) without knowledge of the surgical or postmortem findings.

Computed Tomography (CT)

Computed tomography was performed with a 3rd-generation CT scanner.[e] With the dogs in dorsal recumbency, scans of the abdomen were made from the most cranial part of the liver to a region caudal to the left kidney with a scanning time of 4.5 seconds, 120 kV, 220 mA, and 10- or 5-mm-thick consecutive slices. Scans were made before and after administration in a cephalic vein of 2 mL/kg body weight of sodium and meglumine ioxotalamate[f] IV, with a maximum of 60 mL. Ventilation was controlled manually in all dogs, and scans were made at the end of expiration. CT images were reviewed by 1 of the authors (GV) without knowledge of surgical or postmortem findings. The maximum diameter of all suspected lesions on CT (md-CT) was determined by measuring the lesion on the slice containing the largest cross section and by estimating the craniocaudal dimension from the number of consecutive scans that contained part of the lesion and the slice thickness. The density of all suspected primary and metastatic lesions was measured on both unenhanced and contrast-enhanced images and compared with the density of the liver in each dog. Dimensions and densities were measured from the display monitor with a trackball-driven cursor and CT computer software with images displayed at the same window settings (window width = 400 Hounsfield units, window length = 40 Hounsfield units).

Single Photon Emission Computed Tomography

Six hours before SPECT, a median of 155 MBq (range 56–214 MBq) [^{111}In-DTPA-D-Phe^{1}]-octreotide[g] was injected IV. The synthesis and radiolabeling of the product have been described earlier.[20,21]

SPECT was performed with a single-head gamma camera[h] equipped with a medium-energy parallel-hole collimator. The pulse height analyzer windows were centered over both ^{111}In photon peaks (172 and 246 keV) with a window width of 20%. Data from both windows were added to the acquisition frames. The camera was connected to a dedicated open ICON Workstation computer that used Siemens ICON computer system software. The acquisition time of 64 projections (128- × 128-word matrix) was determined by the number of counts in the 1st segment (90,000–110,000 counts). SPECT images were obtained over 65 minutes. Reconstruction was performed with a Butterworth filter (cutoff 0.35, order 7) without scatter correction. Attenuation correction was performed assuming uniform attenuation with an ellipse drawn around the body. The field of view covered at least the abdomen from the cranial aspect of the diaphragm to the cranial border of the pelvis. In small dogs, a zoom factor of 1.23 was used. SPECT studies of the dogs were reviewed by 1 of the authors (YWEAP) without knowledge of the surgical or postmortem findings.

Descriptive Analysis

The diagnostic imaging techniques were assessed for their value in identifying the primary pancreatic tumor(s), lymph node metastases, and liver metastases. Identification involved not only the detection of a lesion, but also the correct allocation of that lesion to a certain abdominal organ. A result was considered true positive when the primary tumor or lymph node metastases were identified correctly. Results for metastatic liver disease were considered true positive when at least 1 of the liver metastases was correctly identified. A false-positive result was defined as a lesion identified by imaging but not found at surgery or postmortem examination or that was detected but allocated to the wrong organ. A false-negative result by imaging entailed a tumorous lesion that was not detected but found at surgery or postmortem examination or that was detected but located incorrectly. The results are presented as median and range.

Results

Dogs

Thirteen of 16 dogs with insulinoma that initially entered the study met all of the inclusion criteria: 7 were males (1 intact) and 6 were females (2 intact) of 9 different breeds. The median age was 10 years (range 6–11 years), and the median body weight was 22 kg (range 9–36 kg). Recurrent signs of hypoglycemia were present in all dogs before admission. In all dogs, the results of routine clinicopathologic investigations were within the reference range, with the exception of plasma glucose concentrations, which were repeatedly below the lower limit of the reference range (4.0 mmol/L, or 72 mg/dL). Hyperinsulinemia was diagnosed on the basis of low plasma glucose concentrations in the presence of inappropriately high concentrations of plasma insulin (ie, plasma insulin concentrations in the upper range of, or above, the reference range [34–63 pmol/L, or 5.1–9.4 μIU/mL]). Transabdominal US studies were performed a median of 29 days (range 9–42 days) and CT/SPECT studies a median of 14 days (range 3–28 days) before surgery or postmortem examination.

Information on tumor localization and size was obtained at surgery (9 dogs), postmortem examination (1 dog), or both (3 dogs). Twelve dogs had a solitary pancreatic tumor, and 1 dog had 2 pancreatic tumors. Four tumors were located in the right pancreatic lobe, 2 in the pancreatic corpus, and 8 in the left pancreatic lobe. The median md-Control of the primary tumors was 15 mm (range 7–50 mm). One

Table 1. Cumulative descriptive analysis of the results of transabdominal ultrasonography (US), computed tomography (CT), and single-photon emission computed tomography (SPECT) in 13 dogs with insulinoma.

	No. of Lesions[b]					
	Pancreas				Lymph	
Analysis[a]	R (4)	C (2)	L (8)	T (14)	Nodes (5)	Liver (4)
US						
True positive	3	1	1	5	0	2
False positive	1	0	0	1	2	1
False positive*	0	0	2	2	1	0
False negative	1	0	5	6	4	2
False negative*	0	1	0	1	1	0
True negative	—	—	—	—	—	8
CT						
True positive	2	2	6	10	2	2
False positive	0	0	1	1	28	1
False positive*	0	0	1	1	0	0
False negative	2	0	1	3	1	2
False negative*	0	0	0	0	2	0
True negative	—	—	—	—	—	9
SPECT						
True positive	4	0	2	6	0	2
False positive	0	0	0	0	0	0
False positive*	0	0	1	1	0	0
False negative	0	2	5	7	4	2
False negative*	0	0	0	0	1	0
True negative	—	—	—	—	—	9

R, right pancreatic lobe; C, pancreatic corpus; L, left pancreatic lobe; T, whole pancreas.

[a] Asterisks indicate a lesion detected with the imaging technique but localized incorrectly, causing the result to become false positive or false negative.

[b] Numbers in parentheses are number of pancreatic tumor lesions (1 dog had 2 pancreatic lesions), metastatic lymph nodes, or livers with metastases found at surgery or postmortem examination.

dog had 1 pancreaticoduodenal and 1 left hepatic lymph node metastasis; 3 dogs each had 1 metastasis in a splenic lymph node. The 5 lymph node metastases had a median md-Control of 20 mm (range 10–25 mm). Three of the 4 dogs with lymph node metastases also had liver metastases. In 1 dog, multiple subcapsular liver lesions (md-Control range 1–2 mm) were found. Another dog had ~30 liver metastases (md-Control range 1–15 mm). The 3rd dog had 4 liver lesions (md-Control: 2, 5, 14, and 20 mm). In 1 other dog, a solitary liver metastasis (md-Control: 12 mm) was found without lymph node involvement.

The cumulative descriptive analysis for each diagnostic imaging technique is summarized in Table 1, and the results for each tumor lesion found during surgery or postmortem examination are described in Table 2.

Transabdominal Ultrasonography

The quality of the image was poor in 9 of 13 dogs because of gas or other contents in the stomach, duodenum, or colon. In 12 dogs, only parts of the pancreatic region could be identified, and in 1 dog, no pancreas could be visualized at all. Regional lymph nodes were identified only when they had an abnormal hypoechoic structure or were enlarged. Most of the liver could be visualized in all dogs. Primary and lymph node tumor lesions were recognized as round or lobulated, hypoechoic nodules (Fig 1). Metastatic liver lesions were hypoechoic. In 1 dog, the liver lesions had hyperechoic borders.

The median md-Control of 5 pancreatic masses that were correctly identified was 20 mm (range 15–30 mm), whereas the diameter of the 9 unidentified lesions was 15 mm (range 7–50 mm). One lesion (dog 3), considered an enlarged splenic lymph node on US, could well have been an unidentified primary insulinoma on the basis of its size (md-US 26 mm versus md-Control 27 mm) and localization (Table 2). Another mass (dog 12) was identified as primary tumor on US but most likely was a splenic lymph node metastasis on the basis of its size. Both a false-positive and false-negative result were obtained with a primary lesion (dog 13) identified in the right lobe on US, whereas the primary tumor was found in the left pancreatic lobe at surgery and postmortem examination (Tables 1, 2). In the same dog, 2 (md-Control: 10 mm) of ~30 liver metastases were identified on US. In 1 dog, a false-positive finding was due to an irregular liver structure on US that was interpreted as metastatic disease (Table 1). At postmortem examination, hepatocellular nodular hyperplasia was found.

Computed Tomography

In all dogs, lesions that were considered to be primary pancreatic tumors were slightly hypodense compared with liver tissue. The density of these lesions increased after contrast medium injection, either uniformly or irregularly, but the lesions remained slightly hypodense compared with the contrast-enhanced liver tissue. In 11 dogs, 1 or more lymph nodes were identified as round or oval soft tissue structures that uniformly enhanced after contrast medium injection. These lymph nodes were suspected to contain tumor. Liver metastases were visualized as hypodense lesions. In 1 dog, these hypodense lesions were bordered by hyperdense rims.

The median md-Control of the 10 pancreatic lesions that were correctly identified was 20 mm (range 10–50 mm), whereas the diameter of the 4 unidentified lesions was 7, 8, 15, and 25 mm, respectively. One of 2 lesions (dog 1), both allocated to the pancreas, proved to be a left hepatic lymph node metastasis at surgery and postmortem examination. In this dog, CT also identified tumor growth into the portal vein, which was confirmed at surgery and postmortem examination. A primary pancreatic lesion (dog 13) on CT was considered a splenic lymph node in retrospect on the basis of its size (Table 2). In 11 dogs, 30 lymph nodes were identified and considered suspect on CT (median md-CT 10 mm, range 8–40 mm). The majority consisted of left hepatic (n = 7) and splenic (n = 12) lymph nodes. Two of the latter were tumor-positive at surgery or postmortem examination (md-Control: 20 and 10 mm, respectively; Table 1). One liver lesion identified on CT (md-CT: 19 mm) was not associated with the metastatic liver disease present in dog 1. The smallest of the 4 liver metastases in dog 11 (md-Control: 2 mm) was not detected.

Table 2. Descriptive analysis of the results of transabdominal ultrasonography (US), computed tomography (CT), and single-photon emission computed tomography (SPECT) per tumor lesion found during surgery or postmortem examination in 13 dogs with insulinoma.[a]

			Result		
Dog	Lesion	md-Control	US	CT	SPECT
Primary, pancreatic					
1	Left lobe	50	FN[a]	TP	TP
2	Corpus	30	TP	TP	TP
3	Corpus	27	FN*	TP	TP
4	Right lobe	25	TP	FN	FN
5	Right lobe–left lobe[b]	20–15	TP–FN	TP–TP	TP–FN
6	Right lobe	20	TP	TP	FN
7	Left lobe	20	FN	TP	FN
8	Left lobe	15	TP	TP	FN
9	Left lobe	15	FN	TP	TP
10	Right lobe	15	FN	FN	TP
11	Left lobe	10	FN	TP	FN
12	Left lobe	8	FP*	FN	FN
13	Left lobe	7	FN	FP*	FP*
Metastatic, lymph node					
13	Splenic	25	FN	FN*	FN*
12	Splenic	20	FN*	TP	FN
1	Left hepatic	20	FN	FN*	FN
11	Splenic	10	FN	TP	FN
1	Pancreaticoduodenal	10	FN	FN	FN
Metastatic liver disease					
11	4 Lesions	2, 5, 14, 20	FN	TP	TP
13	Multiple lesions	1–15	TP	FN	FN
4	1 Lesion	12	TP	TP	TP
1	Multiple lesions	1–2	FN	FN	FN

[a] md-Control, maximum diameter of lesion(s) as determined at surgery or postmortem examination; TP, true positive; TN, true negative; FP, false positive; FN, false negative. FP* or FN*, a true tumorous lesion detected with the imaging technique but localized incorrectly, causing the result to become false positive or false negative, respectively.

[b] This represents 2 pancreatic lesions in 1 dog.

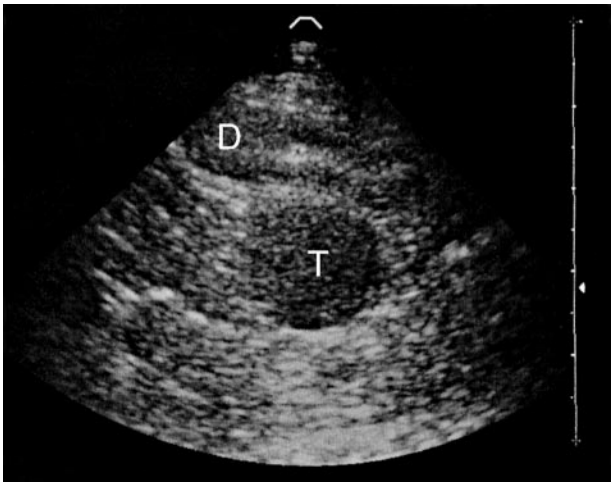

Fig 1. A transverse ultrasound image through the right lateral abdominal wall with the dog in left ventral recumbency (dog 4). A round, hypoechoic mass (T) is visible medial to the duodenum (D). This primary pancreatic tumor was not identified with CT and SPECT. The solitary liver metastasis in this dog was identified with all 3 techniques (Table 2). Distance between tics on the right bar is 0.5 cm.

Single-Photon Emission Computed Tomography

Uptake of radioactivity in the kidneys and gall bladder was readily recognized. The radioactivity in the liver was weak and patchy. All dogs had a circumscribed accumulation of radioactivity in the left epigastrium. Other accumulations of radioactivity on SPECT images differed among dogs but were mainly related to the intestines (Figs 2, 3).

The median md-Control of the 6 pancreatic masses that were correctly identified was 24 mm (range 15–50 mm), whereas the median diameter of the 8 lesions missed was 15 mm (range 7–25 mm). The primary tumors in dogs 5 and 10 were allocated to the pancreatic corpus on SPECT but proved to be present in the right lobe at surgery (Fig 3). A primary lesion (dog 13) identified in the left lobe on SPECT was, in retrospect, more likely to be a closely related splenic lymph node metastasis (Table 2).

The accumulation of radioactivity in the liver (dog 11) was associated with the largest (md-Control 20 mm) of the 4 liver metastases found at postmortem examination. In the same dog, the abnormal distribution of radioactivity related to the gall bladder also could have been caused by the 2nd largest liver metastasis (md-Control: 14 mm). At postmor-

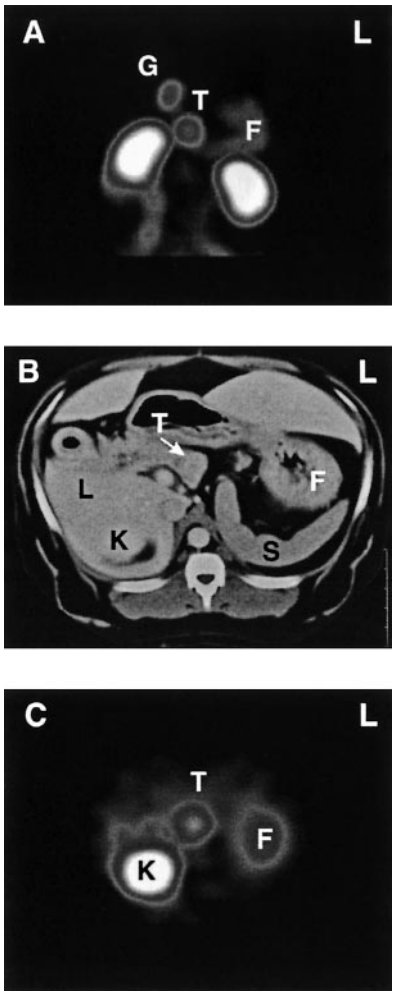

Fig 2. **(A)** A ventral view of a 3-dimensional reconstruction of a SPECT study performed 6 hours after injection of [^{111}In-DTPA-D-Phe^{1}]-octreotide (dog 9). Radioactivity accumulated in kidneys, gall bladder (G), gastric fundus (F), and primary tumor in the left pancreatic lobe (T). Some radioactivity was detected in the intestinal tract. **(B, C)** Corresponding transverse CT and SPECT images, respectively, in the same dog. On the CT image, the right kidney (K), gastric fundus (F), spleen (S), liver (L), and primary tumor (T) can be identified.

Fig 3. **(A)** A ventral view of a 3-dimensional reconstruction of a SPECT study performed 6 hours after injection of [^{111}In-DTPA-D-Phe^{1}]-octreotide (dog 10). Radioactivity accumulated in kidneys, gall bladder (G), and primary tumor in the right pancreatic lobe (T). Some radioactivity was detected in the intestinal tract. **(B, C)** Corresponding transverse CT and SPECT images, respectively, in the same dog. On the CT image, the right kidney (K) and spleen (S) can be identified. The primary tumor was identified on SPECT (T), but only in retrospect; possibly identified on CT (T?).

tem examination, this metastasis was found close to the gall bladder.

Comparison of US, CT, and SPECT

Of the 10 primary tumors identified on CT, 2 (1 in the right pancreatic lobe, 1 in the pancreatic corpus) also were found with SPECT and US, 2 (1 in the right lobe, 1 in the left lobe) with US but not with SPECT, and 3 (1 in the corpus, 2 in the left lobe) with SPECT but not with US (Tables 1, 2). Of the 4 primary tumors not identified with CT, 1 (right lobe) was found with US (Fig 1) and 1 (right lobe) with SPECT only (Fig 3). Two primary tumors (left lobe; md-Control: 7 and 8 mm, respectively) were not detected by any of the imaging techniques. Of the 5 lymph node metastases, only 2 were correctly identified with CT. Two splenic lymph nodes and 1 left hepatic lymph node metastasis were detected with different imaging modalities but misinterpreted as primary tumors in the left lobe. The solitary liver metastasis in 1 dog was identified with all techniques (Table 2). CT and SPECT identified metastases in 1 other dog, whereas US was the only technique to visualize metastases in a 3rd dog. Small metastases (md-Control range 1–2 mm) in the 4th dog were missed with all techniques.

Discussion

Surgical excision is the treatment choice for insulinomas in dogs despite the presence of metastatic disease in 40–50% of affected dogs.[2] Preoperative imaging is necessary to select candidates for surgery, to plan surgery, and to be able to inform owners about the risk of loss of pancreatic function, the chance of therapeutic success, and the extent of surgery.[22]

The accuracy of US depends on the experience of the operator, the size of the lesion, and the quality of the sonograms. Bowel gas and obesity are the most common causes of poor-quality transabdominal sonograms and resultant failure to image the pancreas in humans.[23,24] Additionally, image quality in the dogs in this study was negatively influenced by restlessness, body conformation with a deep chest, and intestinal content. Poor image quality was the main reason why few primary tumors (especially in the left lobe) and lymph node metastases were detected by US. Withholding food, anesthesia, and gastric intubation to remove gas from the stomach and to administer water or saline all could have improved the results of US. However, US in these dogs was performed as part of the routine diagnostic evaluation, even before a definite diagnosis of insulinoma was made. Because withholding food and anesthesia pose an increased risk in dogs with hypoglycemia, US was performed in these dogs without specific preparation.

Thus, we found US to have low sensitivity in detecting canine insulinoma. In a retrospective study, the detection of pancreatic neoplasia in dogs by transabdominal US was reported to be 75% (12/16 dogs).[7] Thirteen of these 16 dogs had insulinomas, and in 4 of these dogs, the tumor was not detected. In no more than 6 dogs, the tumor was detected and accurately localized, whereas the other dogs were considered to have ''probable pancreatic masses.'' The detection and accurate localization of the primary insulinoma in 6 of 13 dogs is comparable to our findings in 5 of 13 dogs. In human medicine, the sensitivity of transabdominal US for the detection of insulinomas varies between 9 and 79%.[25] This variation could reflect improved quality of sonographic equipment over the years, differences in study design, differences in the experience of the examiners, variation in types of neuroendocrine tumors, and small patient groups. Nevertheless, US is readily available, noninvasive, and relatively inexpensive. Ultrasound-guided percutaneous biopsy also might identify the lesion. Despite low sensitivity in the detection of insulinomas, transabdominal US still might be useful for initial assessment of dogs with hypoglycemia and for the exclusion of differential diagnoses of hypoglycemia such as insulinlike growth factor II–like peptide-producing extra-pancreatic tumors.[26]

To our knowledge, this is the 1st report on the use of CT in dogs with insulinoma. CT identified most primary insulinomas (10/14). In humans, the sensitivity of CT for the localization of primary insulinoma depends on tumor size.[27,28] Small tumors might not distort the contour of the human pancreas and could be missed because their attenuation is similar to that of normal pancreatic parenchyma on both pre- and postcontrast scans. In this respect, the relatively thin pancreas in dogs might be advantageous. However, the thin pancreas also could explain why it was difficult to correctly allocate a lesion to either the pancreas or an adjacent lymph node on US and CT imaging.

Variation in the size and number of unaffected lymph nodes and inability to distinguish tumorous from nontumorous enlargement of lymph nodes on CT precluded a definitive diagnosis of metastatic lymph node disease. Because not all lymph nodes could be visualized, lymph nodes that were detected with CT were considered to contain metastases, which resulted in many (28) false-positive findings. This result suggests that CT might not be appropriate for identifying lymph node metastases. In humans with gastrinomas, CT better detects pancreatic lesions (80%) than extrapancreatic, extrahepatic lesions (35%).[11] CT was not better than US or SPECT in detecting metastatic liver disease. New techniques, such as spiral CT, with dual phase contrast enhancement, have improved the sensitivity of detection of PETs in humans compared with conventional CT (85 versus 16–72%).[25,29] The introduction of these techniques to veterinary medicine also could improve the accuracy of the identification of canine insulinoma.

When assessing imaging techniques for the detection of PETs in humans, a distinction is made between primary tumor and metastatic disease.[12] Intraoperative manual palpation and intraoperative US have proven very accurate in identifying primary insulinomas in humans (sensitivity 90–100%).[10,27,28,30,31] Also in our study, all primary insulinomas were found by careful inspection and palpation of the pancreas. Additionally, intraoperative US can detect where the insulinoma lies in relation to the pancreatic duct, common bile duct, and adjacent blood vessels, providing the surgeon with important information. Given the low sensitivity of preoperative imaging techniques (including SRS[14]) in humans with insulinoma, it has been questioned whether preoperative imaging is useful at all.[10,32] In answering this question, it should be remembered that insulinomas are benign in about 90% of human patients, and preoperative imaging is used mainly to detect relatively small, primary pancreatic tumors. The detection of metastatic disease is of less importance.

Numerous imaging methods have been used to assess the extent of metastatic disease in humans with PETs.[11,22,33–35] SRS has become the primary diagnostic imaging technique for the identification and staging of malignant PETs in humans[9–12,14] and is considered more sensitive in detecting metastases than conventional US and CT.[11,13,14]

Lesion detection with SRS depends on the accumulation of radioactivity, which is determined primarily by the size of the lesion and the density of somatostatin receptors.[36] The primary tumors detected in this study were relatively small (md-Control $\leq$ 2 cm in 10/14) compared with malignant PETs such as pancreatic gastrinomas (2–3 cm).[14,37] Therefore, the poor to moderate performance of SRS in dogs with insulinomas could be related to the size of the tumors, but also to a low density of high-affinity somatostatin receptors, as demonstrated in about 40% of insulinomas in humans.[11,37,38] However, preliminary data indicate that most insulinomas in dogs possess sufficient numbers of high-affinity somatostatin receptors for visualization.[19] A 3rd aspect that might have influenced the SPECT detection of primary tumors and metastases in dogs was the nonspecific accumulation of radioactivity in the gall bladder, kidneys, and gastrointestinal tract. In humans, a low-fiber diet and use of laxatives before SRS or SRS performed shortly ($<$4–6 hours) after administration of the radiopharmaceutical can reduce this nonspecific accumulation of radioactivity.[39] Furthermore, tumor-related hot spots can be distinguished from nonspecific bowel radioactive accumulation by repeating SRS after a certain interval.[13,14] In dogs, these measures have practical limitations, such as increased risk

of fasting and additional general anesthesia. Moreover, recent findings suggest that a considerable amount of radioactivity is retained in the gastric and intestinal wall in dogs, which could limit the effectiveness of these measures.[40]

Transabdominal US and CT provide information on anatomical relations and the location of lesions, whereas SRS characterizes the lesion.[12,41] Thus, with the combination of US or CT with SPECT, the detection, localization, and staging of the tumor could be improved. SPECT appears to be as effective as US and CT in detecting primary insulinomas and metastases. However, the combination of imaging modalities, in terms of detection rate, was only slightly better than the individual imaging modalities.

We propose a preliminary protocol for the identification and staging of insulinomas in dogs on the basis of the results of this study and studies of human patients. Transabdominal US could be used for the differential diagnosis and initial assessment (especially for liver metastases). Intraoperative inspection and palpation is preferred for the identification of the primary tumor, but CT could be considered for additional preoperative evaluation. Intraoperative US could become a useful additional approach for detecting primary tumors. With improvements in study protocols and techniques, the combination of US, CT, and SRS could provide improved preoperative information about tumor status.

Footnotes

[a] Domitor, SmithKline Beecham Animal Health B.V., Zoetermeer, The Netherlands
[b] Diprivan, Zeneca B.V., Ridderkerk, The Netherlands
[c] Forene, Abbott Laboratories B.V., Maarsen, The Netherlands
[d] HDI 3000, Advanced Technology Laboratories, Woerden, The Netherlands
[e] Tomoscan CX/S, Philips NV, Eindhoven, The Netherlands
[f] Telebrix 350 (350 mg iodine/mL), Guerbet Nederland B.V., Gorinchem, The Netherlands
[g] OctreoScan, Mallinckrodt Medical B.V., Petten, The Netherlands
[h] Integrated ORBITER Gamma Camera, Siemens Medical Systems, Hoffman Estates, Illinois, USA

Acknowledgments

The studies were performed at the Departments of Clinical Sciences of Companion Animals, Diagnostic Imaging and Pathology of the Faculty of Veterinary Medicine, Utrecht University, Utrecht, The Netherlands. We thank Mallinckrodt Medical B.V., Petten, The Netherlands, for their generous donation of [^{111}In-DTPA-D-Phe^{1}]-octreotide. We acknowledge the support of the staff of the Anesthesiology Division of the Faculty of Veterinary Medicine, Utrecht University, Utrecht, The Netherlands.

References

1. Gross TL, O'Brien TD, Davies AP, Long RE. Glucagon-producing pancreatic endocrine tumors in two dogs with superficial necrolytic dermatitis. J Am Vet Med Assoc 1990;197:1619–1622.

2. Leifer CE, Peterson ME, Matus RE. Insulin-secreting tumor: Diagnosis and medical and surgical management in 55 dogs. J Am Vet Med Assoc 1986;188:60–64.

3. Simpson KW, Dykes NL. Diagnosis and treatment of gastrinoma. Sem Vet Med Surg (Small Anim) 1997;12:274–281.

4. Caywood DD, Klausner JS, O'Leary TP, et al. Pancreatic insulin-producing secreting neoplasms: Clinical, diagnostic, and prognostic features in 73 dogs. J Am Anim Hosp Assoc 1988;24:577–584.

5. Trifonidou MA, Kirpensteijn J, Robben JH. A retrospective evaluation of 51 dogs with insulinoma. Vet Q 1998;20:S114–S115.

6. Feldman EC, Nelson RW. Canine and Feline Endocrinology and Reproduction, 2nd ed. Philadelphia, PA: WB Saunders; 1996:422–441.

7. Lamb CR, Simpson KW, Boswood A, Matthewman LA. Ultrasonography of pancreatic neoplasia in the dog: A retrospective review of 16 cases. Vet Rec 1995;137:65–68.

8. Mantis P, Lamb CR. Sensitivity of ultrasonography for canine insulinomas. Proceedings of the 6th Annual Conference of the European Association of Veterinary Diagnostic Imaging, Vienna, Austria, 1999:40.

9. Angeli E, Vanzulli A, Gastrucci M, et al. Value of abdominal sonography and MR imaging at 0.5 T in preoperative detection of pancreatic insulinoma: A comparison with dynamic CT and angiography. Abdom Imaging 1997;22:295–303.

10. Hashimoto LA, Walsh RM. Preoperative localization of insulinomas is not necessary. J Am Coll Surg 1999;189:368–373.

11. Modlin IM, Tang LH. Approaches to the diagnosis of gut neuroendocrine tumors: The last word (today). Gastroenterology 1997; 112:583–590.

12. Ricke J, Klose K-J. Imaging procedures in neuroendocrine tumours. Digestion 2000;62:39–44.

13. Chiti A, Fanti S, Savelli G, et al. Comparison of somatostatin receptor imaging, computed tomography and ultrasound in the clinical management of neuroendocrine gastro-entero-pancreatic tumours. Eur J Nucl Med 1998;25:1396–1403.

14. Gibril F, Jensen RT. Comparative analysis of diagnostic techniques for localization of gastrointestinal neuroendocrine tumors. Yale J Biol Med 1997;70:509–522.

15. Gibril F, Reynolds JC, Chen CC, et al. Specificity of somatostatin receptor scintigraphy: A prospective study and effects of false-positive localizations on management in patients with gastrinomas. J Nucl Med 1999;40:539–553.

16. Krenning EP, Kooij PPM, Pauwels S, et al. Somatostatin receptor: Scintigraphy and radionuclide therapy. Digestion 1996;57(Suppl): 57–61.

17. Altschul M, Simpson KW, Dykes NL, et al. Evaluation of somatostatin analogues for the detection and treatment of gastrinoma in a dog, J Small Anim Pract 1997;38:286–291.

18. Lester NV, Newell SM, Hill RC, Lanz OI. Scintigraphic diagnosis of insulinoma in a dog. Vet Radiol Ultrasound 1999;40:174–178.

19. Robben JH, Visser-Wisselaaar HA, Rutteman GR, et al. In vitro and in vivo detection of functional somatostatin receptors in canine insulinomas. J Nucl Med 1997;38:1036–1042.

20. Bakker WH, Albert R, Bruns C, et al. [^{111}In-DTPA-D-Phe^{1}]-octreotide, a potential radiopharmaceutical for imaging of somatostatin receptor-positive tumors: Synthesis, radiolabeling and in vitro validation. Life Sci 1991;49:1583–1591.

21. Krenning EP, Bakker WH, Kooij PPM, et al. Somatostatin receptor scintigraphy with indium-111-DTPA-D-Phe-1-octreotide in man: Metabolism, dosimetry and comparison with iodine-123-Tyr-3-octreotide. J Nucl Med 1992;33:652–658.

22. Goldstone AP, Scott-Coombes DM, Lynn JA. Surgical management of gastrointestinal endocrine tumours. Bailliere's Clin Gastroenterol 1996;10:707–736.

23. Kolmannskog F, Swensen T, Vatn MH, Larsen S. Computed tomography and ultrasound of the normal pancreas. Acta Radiol Diagn 1982;23:443–451.

24. Miller DL. Localization of islet cell tumors. In: Becker KL, ed. Principles and Practice of Endocrinology and Metabolism, 3rd ed. Philadelphia, PA: Lippincott, Williams and Wilkins; 2001:1477–1482.

25. Chatziioannou A, Kehagias D, Mourikis D, et al. Imaging and localization of pancreatic insulinomas. J Clin Imaging 2001;25:275–283.

26. Boari A, Barreca A, Bestetti GE, et al. Hypoglycemia in a dog with leiomyoma of the gastric wall producing an insulin-like growth factor II–like peptide. Eur J Endocrinol 1995;143:744–750.

27. Boukhman MP, Karam JM, Shaver J, et al. Localization of insulinoma. Arch Surg 1999;134:818–823.

28. Kuzin NM, Egorov AV, Kondrashin SA, et al. Preoperative and intraoperative topographic diagnosis of insulinoma. World J Surg 1998;22:593–598.

29. King AD, Ko GTC, Yeung VTF, et al. Dual phase spiral CT in the detection of small insulinomas of the pancreas. Br J Radiol 1998; 71:20–23.

30. Lo, C-Y, Lam, K-Y, Kung AWC, et al. Pancreatic insulinomas. A 15-year experience. Arch Surg 1997;132:926–930.

31. Machado MCC, Monteiro da Cunha, JE, Jukemura J, et al. Insulinoma: Diagnostic strategies and surgical treatment. A 22-year experience. Hepatogastroenterology 2001;48:854–858.

32. Azimuddin K, Chamberlain RS. The surgical management of pancreatic neuroendocrine tumors. Surg Clin North Am 2001;81:511–525.

33. Bliss RD, Carter PB, Lennard TWJ. Insulinoma: A review of current management. Surg Oncol 1997;6:49–59.

34. Anderson MA, Carpenter S, Thompson NW, et al. Endoscopic ultrasound is highly accurate and directs management in patients with neuroendocrine tumors of the pancreas. Am J Gastroenterol 2000;95: 2271–2277.

35. Baba Y, Miyazono N, Nakajo M, et al. Localization of insulinomas. Comparison of conventional arterial stimulation with venous sampling (ASVS) and superselective ASVS. Acta Radiol 2000;41; 172–177.

36. Öhrvall Ul, Westlin J-E, Nilsson S, et al. Human biodistribution of [^{111}In]diethyltriaminepentaacetic acid-(DTPA)-D-[Phe^{1}]-octreotide and peroperative detection of endocrine tumors. Cancer Res 1995; 55(Suppl):5794s–5800s.

37. Zimmer T, Stölzel U, Bäder M, et al. Endoscopic ultrasonography and somatostatin receptor scintigraphy in the pre-operative localisation of insulinomas and gastrinomas. Gut 1996;39:562–568.

38. Lamberts SWJ, Krenning EP, Reubi J-C. The role of somatostatin and its analogs in the diagnosis and treatment of tumors. Endocrinol Rev 1991;12:450–482.

39. Leners N, Jamar F, Fiasse R, et al. Indium-111-pentetreotide uptake in endocrine tumors and lymphoma. J Nucl Med 1996;37:916–922.

40. Robben J, Reubi JC, Pollak Y, Voorhout G. Biodistribution of [^{111}In-DTPA-D-Phe^{1}] octreotide in dogs: Uptake in the stomach and intestines but not in the spleen points towards interspecies differences. Nucl Med Biol 2003;30:225–232.

41. Debray MP, Geoffroy O, Laissy JP, et al. Imaging appearances of metastases from neuroendocrine tumours of the pancreas. Br J Radiol 2001;74:1065–1070.